Radio Science, Volume ???, Number , Pages 1–12,

Exact radiation of a dipole in the presence of a circular aperture in a ground plane backed by a spheroidal cavity and covered with an isorefractive diaphragm

M. Valentino

Department of Electrical and Computer Engineering, University of Illinois at Chicago, Chicago, Illinois, USA

D. Erricolo

Department of Electrical and Computer Engineering, University of Illinois at Chicago, Chicago, Illinois, USA

An oblate semi-spheroidal cavity with metallic walls flush-mounted under a metallic ground plane is coupled to the half-space above the ground plane through an aperture that corresponds to the interfocal disk of the oblate spheroidal system. A diaphragm is located across the aperture. The diaphragm material, the material filling the cavity, and the half-space are isorefractive to each other. A new exact solution is obtained for the radiation of an electric or a magnetic dipole located on the symmetry axis of the structure and axially oriented. The exact solution is expressed in terms of series containing oblate spheroidal functions. These series are evaluated to provide a benchmark solution for a primary source located either inside the cavity below the diaphragm, or outside the cavity in the unbounded medium.

1. Introduction

The exact solution to a three-dimensional electromagnetic boundary-value problem involving an oblate semi-spheroidal cavity with metallic walls flush-mounted under a metallic ground plane and coupled to the half-space above the plane via a circular hole is considered. The material above the ground plane is separated from the material inside the cavity by a diaphragm. All materials are isorefractive to each other.

The primary source is an electric or a magnetic dipole located on the axis of symmetry of the structure and axially oriented. The analysis is performed in the frequency domain and the time-dependence factor $\exp(-i\omega t)$ is omitted throughout. The exact solution is written in the form of series expansions involving oblate spheroidal wave functions. The expansion coefficients in the series are analytically determined by imposing the boundary conditions, thereby leading to a canonical solution of the boundary-value problem. The notation for the spheroidal wave functions is that of *Flammer* [1957]. Preliminary results were presented in *Erricolo et al.* [2005d], obtained with a solution technique that extends the one used in *Berardi et al.* [2004]. This technique requires an isorefractive body (see *Uslenghi* [1997a]) and rotational symmetry. Rotational symmetry is required because, in the oblate spheroidal coordinate system, the only known series expansion of an incident field is that of a dipole located along the axis of rotation, with the dipole oriented parallel to the axis (see *Bowman et al.* [1987]). Therefore, another usually simple form of the incident field, plane wave, is not considered because an analytical determination of the modal expansion coefficients cannot be obtained.

This geometry models the penetration of electromagnetic radiation into a cavity or the radiation that escapes from a cavity. The diaphragm represents a mechanical cover that protects the cavity, similar to a radome for a radar antenna.

This paper is organized as follows. The geometry of the problem is discussed in Section 2. The analysis for the electric dipole excitation is given in Section 3, while the analysis for the magnetic dipole is presented in Section 4. In Section 5, numerical results based on the evaluation of the series of oblate spheroidal functions are provided for the fields inside the cavity, inside the diaphragm and in the open space above the structure. Issues such as the evalu-

0048-6604/11/$11.00

ation of the fields and surface currents near the edge of the cavity, and the effect of the diaphragm presence are analyzed in detail. Conclusions are given in Section 4.

There are two main contributions from this paper. First, the exact solution of this complicated problem, which involves a sharp metallic edge, a cavity, and a curved surface separating different penetrable media is provided and it enriches the catalog of available canonical solutions. Second, the evaluation of this new solution provides a benchmark for the validation of frequency-domain electromagnetic computational software.

2. Geometry of the Problem

With reference to the Cartesian coordinates (x, y, z), the geometry of the problem is symmetric with respect to the z axis and it is shown in cross section in Fig. 1.

The various boundaries correspond to coordinate surfaces of the oblate spheroidal coordinate system, with foci located at points A and B, whose distance is the interfocal distance d. The oblate spheroidal coordinates (η, ξ, φ) are a right-handed system related to Cartesian coordinates by:

$$\begin{cases} x = \dfrac{d}{2}\sqrt{(1-\eta^2)(1+\xi^2)}\cos\varphi \\ y = \dfrac{d}{2}\sqrt{(1-\eta^2)(1+\xi^2)}\sin\varphi \\ z = \dfrac{d}{2}\xi\eta \end{cases} \tag{1}$$

where $0 \le \xi < \infty, -1 \le \eta \le 1, 0 \le \varphi \le 2\pi$. The inverse transformation is available in *Berardi et al.* [2004]. However, it is convenient to notice that, in the limit when the interfocal distance d is zero, the oblate spheroidal coordinates reduce to the spherical coordinates; on the other hand, when d is finite, the coordinate surface ξ = constant becomes spherical as ξ approaches infinity:

$$\frac{1}{2}d\xi \to r, \quad \eta \to \cos\theta, \qquad \text{as } \xi \to \infty, \tag{2}$$

where r and θ are spherical coordinates.

The surface $\eta = 0$ is metallic and corresponds to the plane $z = 0$ without the circular focal disk of diameter d. Below the aperture there is a cavity that is limited by a metallic boundary located on an oblate semi-spheroid at $\xi = \xi_1$. Across the aperture is located a diaphragm, which is made of two different isorefractive materials and limited by the surfaces $\xi = \xi_2$ and $\xi = \xi_3$ below and above the aperture, respectively. Both the circular aperture and the diaphragm provide the coupling between the cavity and the unbounded medium.

In general, the surfaces $|\eta|$ = constant represent hyperboloids of revolution with z as the symmetry axis, $\eta > 0$ ($\eta < 0$) for $z > 0$ ($z < 0$), and asymptotic cone of semi-aperture $\theta = \arccos\eta$; in particular, $\eta = 1$ is the positive z-axis, whereas $\eta = -1$ represents the negative z-axis. The surface φ = constant is a half-plane originating in the z axis.

Four different media are considered in this problem, as shown in Fig. 1: the unbounded medium with dielectric permittivity ϵ_1 and magnetic permeability μ_1; the diaphragm that is made of material with parameters ϵ_3, μ_3 for $z > 0$ and ϵ_4, μ_4 for $z < 0$; and the cavity with parameters ϵ_2 and μ_2. Since the media are isorefractive, they have the same propagation constant

$$k = \omega\sqrt{\epsilon\mu} = \omega\sqrt{\epsilon_h\mu_h}, \qquad h = 1, ..., 4; \tag{3}$$

however, in general, they have different intrinsic impedances

$$Z_l = \frac{1}{Y_l} = \sqrt{\frac{\mu_l}{\epsilon_l}} \neq Z_m; \quad l, m = 1, ..., 4, \;\; l \neq m. \tag{4}$$

The notion of *isorefractive* material was introduced by *Uslenghi* [1997b] and is an extension of the notion of *diaphanous* material, e.g. *Jones* [1986]. Isorefractive or diaphanous bodies were considered to study diffraction from wedges by *Knockaert*

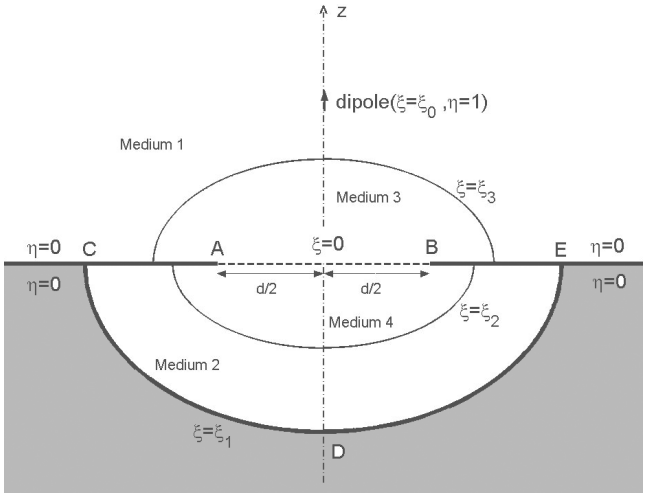

Figure 1. Cross section of the geometry of the problem.

et al. [1997], *Daniele and Uslenghi* [1999], *Uslenghi* [2000], *Uslenghi* [2004b], two dimensional structures including elliptic and parabolic cylinders by *Uslenghi* [1997b] and various semielliptical cavities by *Uslenghi* [2004a], *Erricolo and Uslenghi* [2004], *Erricolo et al.* [2005b], *Erricolo et al.* [2005a], *Erricolo et al.* [2005c], *Valentino and Erricolo* [2006], and three dimensional structures, including prolate and oblate spheroids, paraboloids, circular cones by *Uslenghi and Zich* [1998], *Roy and Uslenghi* [1997], *Erricolo and Uslenghi* [2004], *Erricolo and Uslenghi* [2005a], *Erricolo and Uslenghi* [2005b].

3. Electric Dipole: Analytical Results

As first case, the excitation of the oblate spheroidal cavity is due to an infinitesimal electric dipole or Hertz dipole. The source is located on the axis of symmetry of the structure and it is axially oriented; its moment is given by $\widehat{z}4\pi\epsilon/k$, which corresponds to an electric superpotential or Hertzian vector $\underline{\Pi}^{(e)} = \widehat{z}\exp(ikR)/(kR)$, where R is the distance of the observation point (η, ξ, φ) from the dipole. The electric and magnetic fields generated are of the following form everywhere:

$$\overrightarrow{E} = E_\xi(\eta,\xi)\widehat{\xi} + E_\eta(\eta,\xi)\widehat{\eta}, \qquad E_\varphi = 0; \tag{5}$$

$$\overrightarrow{H} = H_\varphi(\eta,\xi)\widehat{\varphi}, \qquad H_\xi = H_\eta = 0. \tag{6}$$

It is apparent that all the electric field components may be determined by applying Maxwell's equations, once the $\varphi-$component of the magnetic field is known

$$E_\xi = -\frac{iZ}{c}\sqrt{\frac{1-\eta^2}{\xi^2+\eta^2}}\left(\frac{\partial}{\partial\eta} - \frac{\eta}{1-\eta^2}\right)H_\varphi, \tag{7}$$

$$E_\eta = \frac{iZ}{c}\sqrt{\frac{\xi^2+1}{\xi^2+\eta^2}}\left(\frac{\partial}{\partial\xi} + \frac{\xi}{\xi^2+1}\right)H_\varphi, \tag{8}$$

where $c = kd/2$ is the product of the wavenumber and the interfocal radius, and Z is the intrinsic impedance of the medium where the source is located. Furthermore, according to *Bowman et al.* [1987], the primary field generated by an electric dipole can be expanded as a series involving spheroidal wave functions

$$H^i_\varphi = \frac{2k^2Y}{\sqrt{\xi_0^2+1}}\sum_{n=1}^{\infty}\frac{(-i)^n S_{1,n}(-ic,\eta)}{\widetilde{\rho}_{1,n}\widetilde{N}_{1,n}}\times R^{(1)}_{1,n}(-ic,i\xi_<)R^{(3)}_{1,n}(-ic,i\xi_>), \tag{9}$$

where c is constant throughout the structure (because the materials are isorefractive), and Y is the intrinsic admittance of the medium where the field is evaluated. Using the notation of *Flammer* [1957], $S_{1,n}$ is the angular oblate spheroidal function of order 1 and degree n, $R^{(1),(3)}_{1,n}$ are the radial oblate spheroidal functions of order 1, degree n, and of the first and third kind, and $\xi_<$ ($\xi_>$) is the smaller (larger) between ξ and ξ_0.

3.1. Electric Dipole in the Unbounded Medium

When the primary source is a Hertz dipole located at $(1, \xi_0)$ in the unbounded medium, the expression of the incident magnetic field $H^i_{1\varphi}$ is given by (9) with the generic intrinsic admittance Y replaced by Y_1. The total magnetic field in the unbounded medium may be written as sum of three quantities

$$H_{1\varphi} = H^i_{1\varphi} + H^r_{1\varphi} + H^d_{1\varphi}, \tag{10}$$

where $H^r_{1\varphi}$ is the field reflected by the ground plane $z = 0$ (without the aperture and the diaphragm), and the term $H^d_{1\varphi}$ is the perturbation field introduced by the presence of the cavity and the isorefractive diaphragm. By applying image theory, the effect of an electric dipole vertically located above a ground plane is equivalent to the sum of the field of the original dipole and the field of another dipole located symmetrically with respect to the ground plane but in absence of the ground plane. Therefore, the field $H^r_{1\varphi}$ produced at the observation point (η, ξ) by the image dipole ends up being identical to the field generated by the original dipole at $(-\eta, \xi)$:

$$H^r_{1\varphi}(\eta,\xi) = H^i_{1\varphi}(-\eta,\xi). \tag{11}$$

The total geometrical optics field in medium 1 is then expressed as :

$$H^i_{1\varphi} + H^r_{1\varphi} = \frac{-4ik^2Y_1}{\sqrt{\xi_0^2+1}}\sum_{l=0}^{\infty}\frac{(-1)^l S_{1,2l+1}(-ic,\eta)}{\widetilde{\rho}_{1,2l+1}\widetilde{N}_{1,2l+1}}\times R^{(1)}_{1,2l+1}(-ic,i\xi_<)R^{(3)}_{1,2l+1}(-ic,i\xi_>), \tag{12}$$

where some special values for the angular oblate functions (see *Berardi et al.* [2004], Appendix) were used. The diffracted field $H^d_{1\varphi}$ is written as

$$H^d_{1\varphi} = \frac{-4ik^2Y_1}{\sqrt{\xi_0^2+1}}\sum_{l=0}^{\infty}\frac{(-1)^l S_{1,2l+1}(-ic,\eta)}{\widetilde{\rho}_{1,2l+1}\widetilde{N}_{1,2l+1}}\times \left[a^{(e)}_{1l}R^{(3)}_{1,2l+1}(-ic,i\xi)\right], \tag{13}$$

where the presence of radial function of the third kind guarantees that the diffracted field satisfies the

radiation condition, while the modal coefficient $a_{1l}^{(e)}$ is introduced to account for the effect of the presence of the cavity and the diaphragm.

The general expression for the total magnetic field in the other media is given by a linear combination of radial functions of the first and third kind:

$$H_{h\varphi} = \frac{-4ik^2 Y_h}{\sqrt{\xi_0^2+1}} \sum_{l=0}^{\infty} \frac{(-1)^l S_{1,2l+1}(-ic,\eta)}{\widetilde{\rho}_{1,2l+1}\widetilde{N}_{1,2l+1}} \times \left[a_{hl}^{(e)} R_{1,2l+1}^{(3)}(-ic,i\xi) + b_{hl}^{(e)} R_{1,2l+1}^{(1)}(-ic,i\xi)\right], \tag{14a}$$

$$H_{2\varphi} = \frac{-4ik^2 Y_2}{\sqrt{\xi_0^2+1}} \sum_{l=0}^{\infty} \frac{(-1)^l S_{1,2l+1}(-ic,\eta)}{\widetilde{\rho}_{1,2l+1}\widetilde{N}_{1,2l+1}} \times b_{2l}^{(e)} \left[a_{2l}^{(e)} R_{1,2l+1}^{(3)}(-ic,i\xi) + R_{1,2l+1}^{(1)}(-ic,i\xi)\right], \tag{14b}$$

where $h = 3, 4$.

The coefficients $a_{1l}^{(e)}$, $a_{3l}^{(e)}$, $b_{3l}^{(e)}$, $a_{4l}^{(e)}$, $b_{4l}^{(e)}$, $a_{2l}^{(e)}$, $b_{2l}^{(e)}$ are determined imposing a vanishing total tangential electric field on the metallic surfaces, and the continuity of the total tangential electric and magnetic field across the surfaces separating different penetrable media. That yields an algebraic linear system of seven equations, which is solved using Cramer's rule, giving

$$\begin{cases} a_{rl}^{(e)} = \dfrac{-R_{1,2l+1}^{(3)}(-ic,i\xi_0)\Delta a_{rl}^{(e)}}{\Delta^{(e)}}, & r = 1,\ldots,4; \\ b_{sl}^{(e)} = \dfrac{-R_{1,2l+1}^{(3)}(-ic,i\xi_0)\Delta b_{sl}^{(e)}}{\Delta^{(e)}}, & s = 2,\ldots,4. \end{cases} \tag{15}$$

The expressions for the determinants are reported in Table 1, where the following parameters are used:

$$\zeta_{13} = \frac{Z_1}{Z_3}, \quad \zeta_{34} = \frac{Z_3}{Z_4}, \quad \zeta_{42} = \frac{Z_4}{Z_2}, \tag{16}$$

$$N_{2l+1}(\xi) = \frac{R_{1,2l+1}^{(3)}(-ic,i\xi)}{R_{1,2l+1}^{(1)}(-ic,i\xi)}, \tag{17}$$

$$M_{2l+1}(\xi) = \frac{R_{1,2l+1}^{(1)'}(-ic,i\xi) + \dfrac{\xi}{\xi^2+1} R_{1,2l+1}^{(1)}(-ic,i\xi)}{R_{1,2l+1}^{(3)'}(-ic,i\xi) + \dfrac{\xi}{\xi^2+1} R_{1,2l+1}^{(3)}(-ic,i\xi)}. \tag{18}$$

In the particular case when the isorefractive diaphragm is removed, i.e. $\zeta_{13} = \zeta_{42} = 1$ and $\zeta_{34} = \zeta$, the modal coefficients reduce to the ones already found by *Berardi et al.* [2004]:

$$a_{1l}^{(e)} = a_{3l}^{(e)} = -a_{4l}^{(e)} = \frac{-a_{2l}^{(e)} R_{1,2l+1}^{(1)}(-ic,i0) R_{1,2l+1}^{(3)}(-ic,i\xi_0)}{\zeta R_{1,2l+1}^{(1)}(-ic,i0) + (1+\zeta) a_{2l}^{(e)} R_{1,2l+1}^{(3)}(-ic,i0)}, \tag{19a}$$

$$a_{2l}^{(e)} = -M_{2l+1}(\xi_1), \tag{19b}$$

$$b_{2l}^{(e)} = b_{4l}^{(e)} = \frac{a_{1l}^{(e)}}{M_{2l+1}(\xi_1)}, \tag{19c}$$

$$b_{3l}^{(e)} = R_{1,2l+1}^{(3)}(-ic,i\xi_0). \tag{19d}$$

The diffracted far field can be easily computed recalling the asymptotic form of both the oblate spheroidal coordinates (2), and the radial spheroidal function of the third kind for large values of ξ:

$$H_{1\varphi}^{d}\big|_{c\xi\to\infty} \sim \frac{e^{ikr}}{kr} \frac{4ik^2 Y_1}{\sqrt{\xi_0^2+1}} \sum_{l=0}^{\infty} \frac{a_{1l}^{(e)} S_{1,2l+1}(-ic,\cos\theta)}{\widetilde{\rho}_{1,2l+1}\widetilde{N}_{1,2l+1}}. \tag{20}$$

The fundamental relationship between the induced current density vector $\mathbf{J}$ and the tangential magnetic field on a metallic surface yields:

$$\mathbf{J}|_{\xi=\xi_1} = -\widehat{\xi} \times (H_{2\varphi}\widehat{\varphi})\Big|_{\xi=\xi_1} = -(H_{2\varphi}\widehat{\eta})|_{\xi=\xi_1}, \tag{21a}$$

$$\mathbf{J}|_{\xi_2\le\xi\le\xi_1}^{\eta=0} = -\widehat{\eta} \times (H_{2\varphi}\widehat{\varphi})|_{\eta=0} = \left(H_{2\varphi}\widehat{\xi}\right)\Big|_{\eta=0}, \tag{21b}$$

$$\mathbf{J}|_{0<\xi\le\xi_2}^{\eta=0} = -\widehat{\eta} \times (H_{4\varphi}\widehat{\varphi})|_{\eta=0} = \left(H_{4\varphi}\widehat{\xi}\right)\Big|_{\eta=0}, \tag{21c}$$

$$\mathbf{J}|_{0<\xi\le\xi_3}^{\eta=0} = \widehat{\eta} \times (H_{3\varphi}\widehat{\varphi})|_{\eta=0} = -\left(H_{3\varphi}\widehat{\xi}\right)\Big|_{\eta=0}, \tag{21d}$$

$$\mathbf{J}|_{\xi_3\le\xi<\infty}^{\eta=0} = \widehat{\eta} \times (H_{1\varphi}\widehat{\varphi})|_{\eta=0} = -\left(H_{1\varphi}\widehat{\xi}\right)\Big|_{\eta=0}; \tag{21e}$$

where five different metallic regions are identified. The explicit expression for the induced current density vector is not reported here; however it is available in *Valentino* [2005].

3.2. Electric Dipole in Medium 2

When the excitation of the cavity is provided by an electric dipole located on the z axis at $(-1, \xi_2 < \xi_0 < \xi_1)$ in the material filling the spheroidal cavity, and axially oriented, the solution of the electromagnetic boundary-value problem is similar to the one outlined in Section 3.1.

The total geometrical optics magnetic field in the medium where the source is located, is still given by (12), except for the intrinsic admittance Y_1 that now becomes Y_2. It is also apparent that the scattered field in medium 2 not only contains the radial spheroidal function of the third kind, as in the previous case for $H^d_{1\varphi}$, but also the radial function of the first kind: the medium where the source is located is indeed bounded by the metallic cavity described by the coordinate surface $\xi = \xi_1$, thus requiring a combination of the two linearly independent radial functions. Therefore the expression for the total field in medium 2 is given by:

$$H_{2\varphi} = -\frac{4ik^2Y_2}{\sqrt{\xi_0^2+1}}\sum_{l=0}^{\infty}\frac{(-1)^l S_{1,2l+1}(-ic,\eta)}{\widetilde{\rho}_{1,2l+1}\widetilde{N}_{1,2l+1}}\times \Big[R^{(1)}_{1,2l+1}(-ic,i\xi_<)R^{(3)}_{1,2l+1}(-ic,i\xi_>)+ c^{(e)}_{2l}R^{(3)}_{1,2l+1}(-ic,i\xi)+d^{(e)}_{2l}R^{(1)}_{1,2l+1}(-ic,i\xi)\Big]. \tag{22}$$

On the other hand, the diffracted field in medium 1 is still given by equation (13), where the modal coefficient $a^{(e)}_{1l}$ becomes $c^{(e)}_{1l}$.

In media 3 and 4 the total field coincides with the scattered field, as shown in the following equation, where $h = 3, 4$:

$$H_{h\varphi} = -\frac{4ik^2Y_h}{\sqrt{\xi_0^2+1}}\sum_{l=0}^{\infty}\frac{(-1)^l S_{1,2l+1}(-ic,\eta)}{\widetilde{\rho}_{1,2l+1}\widetilde{N}_{1,2l+1}}\times \Big[d^{(e)}_{hl}R^{(1)}_{1,2l+1}(-ic,i\xi)+c^{(e)}_{hl}R^{(3)}_{1,2l+1}(-ic,i\xi)\Big]. \tag{23}$$

In this case the set of boundary conditions is identical to the one outlined in Section 3.1 and yields

$$\begin{cases} c^{(e)}_{rl} = \dfrac{\Delta c^{(e)}_{rl}}{\Delta^{(e)}}, & r = 1,\dots,4; \\ d^{(e)}_{sl} = \dfrac{\Delta d^{(e)}_{sl}}{\Delta^{(e)}}, & s = 2,\dots,4. \end{cases} \tag{24}$$

where $\Delta^{(e)}$ is given by (59a) and the other determinants are reported in Table 2.

The expression for the magnetic far-field in the unbounded medium is obtained by replacing the modal coefficient $a^{(e)}_{1l}$ by $c^{(e)}_{1l}$ in (20).

The induced current density on the metallic surfaces is still computed by substituting the new expression for the magnetic field in equations (21a) through (21e).

3.3. Electric Dipole in Medium 3

For an electric dipole located on the z axis in medium 3, and axially oriented, the same procedure yields

$$H_{1\varphi} = -\frac{4ik^2Y_1}{\sqrt{\xi_0^2+1}}\sum_{l=0}^{\infty}\frac{(-1)^l S_{1,2l+1}(-ic,\eta)}{\widetilde{\rho}_{1,2l+1}\widetilde{N}_{1,2l+1}}\times \Big[\widetilde{a}^{(e)}_{1l}R^{(3)}_{1,2l+1}(-ic,i\xi)\Big], \tag{25}$$

$$H_{3\varphi} = -\frac{4ik^2Y_3}{\sqrt{\xi_0^2+1}}\sum_{l=0}^{\infty}\frac{(-1)^l S_{1,2l+1}(-ic,\eta)}{\widetilde{\rho}_{1,2l+1}\widetilde{N}_{1,2l+1}}\times \Big[R^{(1)}_{1,2l+1}(-ic,i\xi_<)R^{(3)}_{1,2l+1}(-ic,i\xi_>)+\widetilde{b}^{(e)}_{3l}\times R^{(1)}_{1,2l+1}(-ic,i\xi)+\widetilde{a}^{(e)}_{3l}R^{(3)}_{1,2l+1}(-ic,i\xi)\Big], \tag{26}$$

$$H_{4\varphi} = -\frac{4ik^2Y_4}{\sqrt{\xi_0^2+1}}\sum_{l=0}^{\infty}\frac{(-1)^l S_{1,2l+1}(-ic,\eta)}{\widetilde{\rho}_{1,2l+1}\widetilde{N}_{1,2l+1}}\times \Big[\widetilde{b}^{(e)}_{4l}R^{(1)}_{1,2l+1}(-ic,i\xi)+\widetilde{a}^{(e)}_{4l}R^{(3)}_{1,2l+1}(-ic,i\xi)\Big], \tag{27}$$

$$H_{2\varphi} = -\frac{4ik^2Y_2}{\sqrt{\xi_0^2+1}}\sum_{l=0}^{\infty}\frac{(-1)^l S_{1,2l+1}(-ic,\eta)}{\widetilde{\rho}_{1,2l+1}\widetilde{N}_{1,2l+1}}\widetilde{b}^{(e)}_{2l}\times \Big[R^{(1)}_{1,2l+1}(-ic,i\xi)+\widetilde{a}^{(e)}_{2l}R^{(3)}_{1,2l+1}(-ic,i\xi)\Big]. \tag{28}$$

The application of the boundary condition to the tangential component of the total electric field on the metallic boundary of the cavity at $\xi = \xi_1$ requires that $\widetilde{a}^{(e)}_{2l} = -M_{2l+1}(\xi_1)$, while the other modal coefficients are obtained by imposing the other boundary conditions. The resulting linear system of equations yields

$$\begin{cases} \widetilde{a}^{(e)}_{rl} = \dfrac{\Delta\widetilde{a}^{(e)}_{rl}}{\Delta^{(e)}}, & r = 1,3,4; \\ \widetilde{b}^{(e)}_{sl} = \dfrac{\Delta\widetilde{b}^{(e)}_{sl}}{\Delta^{(e)}}, & s = 2,\dots,4. \end{cases} \tag{29}$$

where the explicit expressions of each determinant (except for $\Delta^{(e)}$ in equation (59a)) is available in Table 3.

3.4. Electric Dipole in Medium 4

When the cavity of Fig. 1 is illuminated by an infinitesimal electric dipole located at $(-1, 0 < \xi_0 < \xi_2)$ in medium 4, the expression for the total magnetic field in the unbounded medium and in the material filling the cavity are given by (25) and (28), where the modal coefficients $\widetilde{a}^{(e)}_{1l}$, $\widetilde{a}^{(e)}_{2l}$ and $\widetilde{b}^{(e)}_{2l}$ are replaced by $\widetilde{c}^{(e)}_{1l}$, $\widetilde{c}^{(e)}_{2l}$ and $\widetilde{d}^{(e)}_{2l}$, respectively. Moreover,

the expressions of the total fields inside the isorefractive media 3 and 4 that constitute the diaphragm are given by, respectively:

$$H_{3\varphi} = -\frac{4ik^2Y_3}{\sqrt{\xi_0^2+1}}\sum_{l=0}^{\infty}\frac{(-1)^l S_{1,2l+1}(-ic,\eta)}{\widetilde{\rho}_{1,2l+1}\widetilde{N}_{1,2l+1}}\times \left[\widetilde{c}_{3l}^{(e)}R_{1,2l+1}^{(3)}(-ic,i\xi)+\widetilde{d}_{3l}^{(e)}R_{1,2l+1}^{(1)}(-ic,i\xi)\right]; \quad (30)$$

$$H_{4\varphi} = -\frac{4ik^2Y_4}{\sqrt{\xi_0^2+1}}\sum_{l=0}^{\infty}\frac{(-1)^l S_{1,2l+1}(-ic,\eta)}{\widetilde{\rho}_{1,2l+1}\widetilde{N}_{1,2l+1}}\times \left[R_{1,2l+1}^{(1)}(-ic,i\xi_<)R_{1,2l+1}^{(3)}(-ic,i\xi_>)+\widetilde{d}_{4l}^{(e)}\times R_{1,2l+1}^{(1)}(-ic,i\xi)+\widetilde{c}_{4l}^{(e)}R_{1,2l+1}^{(3)}(-ic,i\xi)\right]. \quad (31)$$

The general form of the solution to the linear system of equations obtained by imposing the boundary conditions is written as

$$\begin{cases}\widetilde{c}_{rl}^{(e)} = \dfrac{\Delta\widetilde{c}_{rl}^{(e)}}{\Delta^{(e)}}, & r=1,\ldots,4;\\ \widetilde{d}_{sl}^{(e)} = \dfrac{\Delta\widetilde{d}_{sl}^{(e)}}{\Delta^{(e)}}, & s=2,\ldots,4.\end{cases} \quad (32)$$

Since the determinant of the coefficient does not depend upon the location of the source, the expression for $\Delta^{(e)}$ is still equation (59a), whereas the other determinants are presented in Table 4.

4. Magnetic Dipole: Analytical Results

As second case, the oblate semi-spheroidal cavity is illuminated by an infinitesimal magnetic dipole located on the z axis and axially oriented.

The dipole moment of the primary source is $\widehat{z}4\pi/k$ corresponding to a magnetic superpotential vector, or magnetic Hertz vector $\underline{\Pi}^{(m)} = \widehat{z}\exp(ikR)/(kR)$. The reason for the magnetic dipole moment not to depend upon the magnetic permeability μ is simply due to consistency with the classical definition of the magnetization vector.

The field components generated by a magnetic dipole located at $(\pm1,\xi_0)$ in an oblate spheroidal coordinate system are everywhere of the type

$$\overrightarrow{E} = E_\varphi(\eta,\xi)\widehat{\varphi}, \quad E_\xi = E_\eta = 0, \quad (33a)$$

$$\overrightarrow{H} = H_\xi(\eta,\xi)\widehat{\xi} + H_\eta(\eta,\xi)\widehat{\eta}, \quad H_\varphi = 0. \quad (33b)$$

The only magnetic field components of interest are

$$H_\xi = -\frac{i\sqrt{1+\xi^2}}{cZ\sqrt{\xi^2+\eta^2}}\left(\frac{\partial}{\partial\xi}+\frac{\xi}{\xi^2+1}\right)E_\varphi, \quad (34)$$

$$H_\eta = \frac{i\sqrt{1-\eta^2}}{cZ\sqrt{\xi^2+\eta^2}}\left(\frac{\partial}{\partial\eta}-\frac{\eta}{1-\eta^2}\right)E_\varphi. \quad (35)$$

The series expansion for the electric field E_φ generated by a magnetic dipole is given by *Bowman et al.* [1987] as

$$E_\varphi^i = -\frac{2k^2Z}{\sqrt{\xi_0^2+1}}\sum_{n=1}^{\infty}\frac{(-i)^n S_{1,n}(-ic,\eta)}{\widetilde{\rho}_{1,n}\widetilde{N}_{1,n}}\times R_{1,n}^{(1)}(-ic,i\xi_<)R_{1,n}^{(3)}(-ic,i\xi_>). \quad (36)$$

Since the procedure needed for solving the electromagnetic problem when the source is represented by an ideal magnetic dipole is very similar to the one outlined earlier, the analytical details will be skipped.

4.1. Magnetic Dipole in the Unbounded Medium

For a primary magnetic source located at $(1,\xi_3<\xi_0)$, the total electric field in the unbounded medium may be expressed by the sum of the following three components:

$$E_{1\varphi} = E_{1\varphi}^i + E_{1\varphi}^r + E_{1\varphi}^d. \quad (37)$$

$E_{1\varphi}^i$ is the incident electric field given by (36) with $Z = Z_1$. $E_{1\varphi}^r$ is the reflected field due to the $z=0$ ground plane, when both the aperture and the diaphragm are removed. Application of the image theory yields

$$E_{1\varphi}^r(\eta,\xi) = -E_{1\varphi}^i(-\eta,\xi), \quad (38)$$

and, recalling some of the properties of the angular spheroidal functions in *Berardi et al.* [2004], the total geometrical optics field $E_{1\varphi}^i + E_{1\varphi}^r$ is:

$$E_{1\varphi}^i+E_{1\varphi}^r = -\frac{4k^2Z_1}{\sqrt{\xi_0^2+1}}\sum_{l=1}^{\infty}\frac{(-1)^l}{\widetilde{\rho}_{1,2l}\widetilde{N}_{1,2l}}\times R_{1,2l}^{(1)}(-ic,i\xi_<)R_{1,2l}^{(3)}(-ic,i\xi_>)S_{1,2l}(-ic,\eta). \quad (39)$$

$E_{1\varphi}^{(d)}$ is the perturbation term due to the presence of both the cavity and the isorefractive diaphragm.

From a mathematical standpoint, the expression for the geometrical optics electric field in equation (39) is dual to that one shown in (12) for electric dipole illumination, since the spheroidal functions of even degree replace the odd degree functions in the series expansion of the field. However, it should be

stressed that the two problems are not dual according to the electromagnetic theory, since perfect electric conductors are involved in both cases.

In order to determine the total electric field in the unbounded medium, it is needed to introduce the secondary field scattered by the cavity, whose general expression may be given by:

$$E^d_{1\varphi} = -\frac{4k^2 Z_1}{\sqrt{\xi_0^2+1}} \sum_{l=1}^{\infty} \frac{(-1)^l a^{(m)}_{1l}}{\widetilde{\rho}_{1,2l}\widetilde{N}_{1,2l}} \times R^{(3)}_{1,2l}(-ic, i\xi) S_{1,2l}(-ic, \eta), \tag{40}$$

where both the Silver-Müller radiation condition, and the boundary condition on the metallic surface $\eta = 0$ are satisfied.

The total $\varphi-$component of the electric field in the other media can be written as follows

$$E_{h\varphi} = -\frac{4k^2 Z_h}{\sqrt{\xi_0^2+1}} \sum_{l=1}^{\infty} \frac{(-1)^l S_{1,2l}(-ic, \eta)}{\widetilde{\rho}_{1,2l}\widetilde{N}_{1,2l}} \times \left[b^{(m)}_{hl} R^{(1)}_{1,2l}(-ic, i\xi) + a^{(m)}_{hl} R^{(3)}_{1,2l}(-ic, i\xi) \right], \quad h = 3, 4; \tag{41a}$$

$$E_{2\varphi} = -\frac{4k^2 Z_2}{\sqrt{\xi_0^2+1}} \sum_{l=1}^{\infty} \frac{(-1)^l S_{1,2l}(-ic, \eta)}{\widetilde{\rho}_{1,2l}\widetilde{N}_{1,2l}} b^{(m)}_{2l} \times \left[R^{(1)}_{1,2l}(-ic, i\xi) + a^{(m)}_{2l} R^{(3)}_{1,2l}(-ic, i\xi) \right]. \tag{41b}$$

The formulation for the electric field in medium 2 given in equation (41b) is aimed at simplifying the imposition of the boundary condition for the vanishing total tangential electric field on the metallic cavity described by $\xi = \xi_1$. Other six boundary conditions are necessary to determine a unique solution to the modal coefficients. The coupling mechanism from one region to the other is cascaded in the sense that the exterior medium 1 is coupled to medium 2 only through medium 3 and 4. The resulting system of linear equations is sparse and could also be easily solved by hand. Because of the cascaded nature of the coupling mechanism, one could extend this derivation to consider a more complex geometry where, for example, the diaphragm is made of N isorefractive layers.

When solving the linear system of equations originated by the imposition of the boundary conditions, it is convenient to use the same notation as before for the intrinsic impedance ratios and to introduce two auxiliary functions by analogy with the electric dipole case:

$$F_{2l}(\xi) = \frac{R^{(1)'}_{1,2l}(-ic, i\xi) + \dfrac{\xi}{\xi^2+1} R^{(1)}_{1,2l}(-ic, i\xi)}{R^{(3)'}_{1,2l}(-ic, i\xi) + \dfrac{\xi}{\xi^2+1} R^{(3)}_{1,2l}(-ic, i\xi)}; \tag{42a}$$

$$G_{2l}(\xi) = \frac{R^{(1)}_{1,2l}(-ic, i\xi)}{R^{(3)}_{1,2l}(-ic, i\xi)}. \tag{42b}$$

The explicit solution can be written in a compact fashion as follows:

$$\begin{cases} a^{(m)}_{rl} = -R^{(3)}_{1,2l}(-ic, i\xi_0) \dfrac{\Delta a^{(m)}_{rl}}{\Delta^{(m)}}, & r = 1, \ldots, 4; \\ b^{(m)}_{sl} = -R^{(3)}_{1,2l}(-ic, i\xi_0) \dfrac{\Delta b^{(m)}_{sl}}{\Delta^{(m)}}, & s = 2, \ldots, 4. \end{cases} \tag{43}$$

where all the determinants are reported in Table 5.

The diffracted far field can be easily computed recalling the behavior of the oblate spheroidal coordinates (2), and of the radial spheroidal function of the third kind for large values of ξ. The diffracted electric field $E^d_{1\varphi}$ in medium 1 becomes:

$$H^d_{1\varphi}\big|_{c\xi\to\infty} \sim \frac{e^{ikr}}{kr} \frac{4ik^2 Z_1}{\sqrt{\xi_0^2+1}} \sum_{l=1}^{\infty} \frac{a^{(m)}_{1l} S_{1,2l}(-ic, \cos\theta)}{\widetilde{\rho}_{1,2l}\widetilde{N}_{1,2l}}. \tag{44}$$

The analytical expression for the vector current density $\mathbf{J}$ induced on the metallic surfaces is obtained from Maxwell's equations according to the following formulas:

$$\mathbf{J}|_{\xi=\xi_1} = \left(H_{2\eta}\widehat{\varphi}\right)|_{\xi=\xi_1}, \tag{45a}$$

$$\mathbf{J}|^{\eta=0}_{\xi_2\le\xi\le\xi_1} = -\left(H_{2\xi}\widehat{\varphi}\right)|_{\eta=0}, \tag{45b}$$

$$\mathbf{J}|^{\eta=0}_{0<\xi\le\xi_2} = -\left(H_{4\xi}\widehat{\varphi}\right)|_{\eta=0}, \tag{45c}$$

$$\mathbf{J}|^{\eta=0}_{0<\xi\le\xi_3} = \left(H_{3\xi}\widehat{\varphi}\right)|_{\eta=0}, \tag{45d}$$

$$\mathbf{J}|^{\eta=0}_{\xi_3\le\xi<\infty} = \left(H_{1\xi}\widehat{\varphi}\right)|_{\eta=0}. \tag{45e}$$

4.2. Magnetic Dipole in Medium 2

The exact solution for the electromagnetic boundary-value problem when the excitation is provided by a magnetic dipole located at $(-1, \xi_2 < \xi_0 < \xi_1)$ in medium 2 is derived similarly to the procedure outlined in Section 4.1. The geometrical optics field in the medium where the source is located is computed assuming that the metallic wall recedes to infinity ($\xi_1 \to \infty$) and that both the circular hole and the isorefractive diaphragm are removed; the to-

tal geometrical optics contribution is then given by

$$E^i_{2\varphi}+E^r_{2\varphi}=-\frac{4k^2Z_2}{\sqrt{\xi_0^2+1}}\sum_{l=1}^{\infty}\frac{(-1)^l}{\widetilde{\rho}_{1,2l}\widetilde{N}_{1,2l}}R^{(1)}_{1,2l}(-ic,i\xi_<)\times R^{(3)}_{1,2l}(-ic,i\xi_>)S_{1,2l}(-ic,\eta). \quad (46)$$

Since the medium where the source is located is bounded, the scattered field due to the presence of both the metallic oblate semi-spheroidal cavity and the coupling aperture covered by the diaphragm may be written as a series expansion involving a linear combination of radial spheroidal functions of the first and third kind. It is also evident that the total electric field in the materials forming the isorefractive diaphragm may be written using a similar formulation; therefore

$$E_{h\varphi}=-\frac{4k^2Z_h}{\sqrt{\xi_0^2+1}}\sum_{l=1}^{\infty}\frac{(-1)^lS_{1,2l}(-ic,\eta)}{\widetilde{\rho}_{1,2l}\widetilde{N}_{1,2l}}\times\left[d^{(m)}_{hl}R^{(1)}_{1,2l}(-ic,i\xi)+c^{(m)}_{hl}R^{(3)}_{1,2l}(-ic,i\xi)\right],\quad h=3,4. \quad (47)$$

The total electric field in medium 2 is given by the sum of the geometrical optics field and the scattered component in (47) for $h=2$:

$$E_{2\varphi}=-\frac{4k^2Z_2}{\sqrt{\xi_0^2+1}}\sum_{l=1}^{\infty}\frac{(-1)^lS_{1,2l}(-ic,\eta)}{\widetilde{\rho}_{1,2l}\widetilde{N}_{1,2l}}\times\left[R^{(1)}_{1,2l}(-ic,i\xi_<)R^{(3)}_{1,2l}(-ic,i\xi_>)+c^{(m)}_{2l}\times R^{(3)}_{1,2l}(-ic,i\xi)+d^{(m)}_{2l}R^{(1)}_{1,2l}(-ic,i\xi)\right]. \quad (48)$$

Similarly to other cases already examined, the total diffracted field in medium 1 has to satisfy the radiation condition, therefore its series expansion contains the radial function of the third kind only:

$$E_{1\varphi}=-\frac{4k^2Z_1}{\sqrt{\xi_0^2+1}}\sum_{l=1}^{\infty}\frac{(-1)^lc^{(m)}_{1l}}{\widetilde{\rho}_{1,2l}\widetilde{N}_{1,2l}}\times R^{(3)}_{1,2l}(-ic,i\xi)S_{1,2l}(-ic,\eta). \quad (49)$$

The determination of the seven modal coefficients is obtained by imposing the boundary conditions. The resulting linear system of equations is not reported here; however its solution is given by:

$$\begin{cases} c^{(m)}_{rl}=\dfrac{\Delta c^{(m)}_{rl}}{\Delta^{(m)}}, & r=1,\ldots,4;\\ d^{(m)}_{sl}=\dfrac{\Delta d^{(m)}_{sl}}{\Delta^{(m)}}, & s=2,\ldots,4; \end{cases} \quad (50)$$

where $\Delta^{(m)}$ is given by (63a), while the other determinants are presented in Table 6.

Recalling the asymptotic expansion for the radial oblate function of third kind, first order and even degree, the far field in medium 1 is:

$$E^d_{1\varphi}\big|_{c\xi\to\infty}\sim\frac{e^{ikr}}{kr}\frac{2ik^2Z_1}{\sqrt{\xi_0^2+1}}\sum_{l=1}^{\infty}\frac{c^{(m)}_{1l}S_{1,2l}(-ic,\cos\theta)}{\widetilde{\rho}_{1,2l}\widetilde{N}_{1,2l}}. \quad (51)$$

The induced current densities per unit surface may be easily computed replacing the analytical expressions for the magnetic fields in (45a) through (45e).

4.3. Magnetic Dipole in Medium 3

For a magnetic dipole located on the z axis in medium 3, and axially oriented, the expression for the total electric field inside the isorefractive diaphragm is given by:

$$E_{3\varphi}=-\frac{4k^2Z_3}{\sqrt{\xi_0^2+1}}\sum_{l=1}^{\infty}\frac{(-1)^lS_{1,2l}(-ic,\eta)}{\widetilde{\rho}_{1,2l}\widetilde{N}_{1,2l}}\times\left[R^{(1)}_{1,2l}(-ic,i\xi_<)R^{(3)}_{1,2l}(-ic,i\xi_>)+\widetilde{b}^{(m)}_{3l}R^{(1)}_{1,2l}(-ic,i\xi)+\widetilde{a}^{(m)}_{3l}R^{(3)}_{1,2l}(-ic,i\xi)\right], \quad (52a)$$

$$E_{4\varphi}=-\frac{4k^2Z_4}{\sqrt{\xi_0^2+1}}\sum_{l=1}^{\infty}\frac{(-1)^lS_{1,2l}(-ic,\eta)}{\widetilde{\rho}_{1,2l}\widetilde{N}_{1,2l}}\left[\widetilde{b}^{(m)}_{4l}R^{(1)}_{1,2l+1}(-ic,i\xi)+\widetilde{a}^{(m)}_{4l}R^{(3)}_{1,2l}(-ic,i\xi)\right], \quad (52b)$$

in the unbounded medium by:

$$E_{1\varphi}=-\frac{4k^2Z_1}{\sqrt{\xi_0^2+1}}\sum_{l=1}^{\infty}\frac{(-1)^lS_{1,2l}(-ic,\eta)}{\widetilde{\rho}_{1,2l}\widetilde{N}_{1,2l}}\widetilde{a}^{(m)}_{1l}R^{(3)}_{1,2l}(-ic,i\xi), \quad (53)$$

and inside the cavity by

$$E_{2\varphi}=-\frac{4k^2Z_2}{\sqrt{\xi_0^2+1}}\sum_{l=1}^{\infty}\frac{(-1)^lS_{1,2l}(-ic,\eta)}{\widetilde{\rho}_{1,2l}\widetilde{N}_{1,2l}}\widetilde{b}^{(m)}_{2l}\times\left[R^{(1)}_{1,2l}(-ic,i\xi)+\widetilde{a}^{(m)}_{2l}R^{(3)}_{1,2l}(-ic,i\xi)\right]. \quad (54)$$

The modal coefficients are given by:

$$\begin{cases} \widetilde{a}^{(m)}_{rl}=\dfrac{\Delta\widetilde{a}^{(m)}_{rl}}{\Delta^{(m)}}, & r=1,3,4;\\ \widetilde{b}^{(m)}_{sl}=\dfrac{\Delta\widetilde{b}^{(m)}_{sl}}{\Delta^{(m)}}, & s=2,\ldots,4; \end{cases} \quad (55)$$

where $\widetilde{a}^{(m)}_{2l}=-G_{2l}(\xi_1)$, $\Delta^{(m)}$ is given by (63a), and the other determinants are in Table 7.

4.4. Magnetic Dipole in Medium 4

When the cavity in Fig. 1 is illuminated by an infinitesimal magnetic dipole located in medium 4 at $(0 < \xi_0 < \xi_2, -1)$, the expression for the total electric field in both the unbounded medium and in the material filling the cavity are given by (53) and (54),

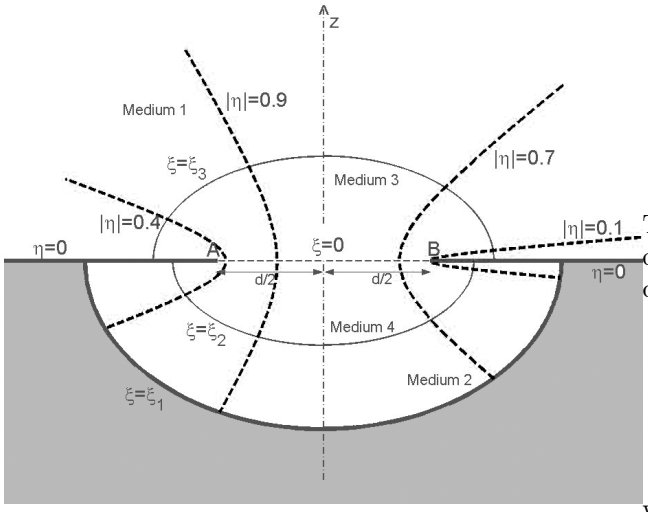

Figure 2. Oblate spheroidal cavity. The dashed hyperbolic curves represent trajectories where the fields are evaluated.

where the modal coefficients $\widetilde{a}_{1l}^{(m)}$, $\widetilde{a}_{2l}^{(m)}$ and $\widetilde{b}_{2l}^{(m)}$ are replaced by $\widetilde{c}_{1l}^{(m)}$, $\widetilde{c}_{2l}^{(m)}$ and $\widetilde{d}_{2l}^{(m)}$, respectively. The total field in the other two media is:

$$E_{3\varphi} = -\frac{4k^2 Z_3}{\sqrt{\xi_0^2+1}} \sum_{l=1}^{\infty} \frac{(-1)^l S_{1,2l}(-ic,\eta)}{\widetilde{\rho}_{1,2l}\widetilde{N}_{1,2l}} \Big[\widetilde{c}_{3l}^{(m)} \times R_{1,2l}^{(3)}(-ic,i\xi) + \widetilde{d}_{3l}^{(m)} R_{1,2l}^{(1)}(-ic,i\xi)\Big], \quad (56a)$$

$$E_{4\varphi} = -\frac{4k^2 Z_4}{\sqrt{\xi_0^2+1}} \sum_{l=1}^{\infty} \frac{(-1)^l S_{1,2l}(-ic,\eta)}{\widetilde{\rho}_{1,2l}\widetilde{N}_{1,2l}} \times \Big[R_{1,2l}^{(1)}(-ic,i\xi_<) R_{1,2l}^{(3)}(-ic,i\xi_>) + \widetilde{d}_{4l}^{(m)} \times R_{1,2l}^{(1)}(-ic,i\xi) + \widetilde{c}_{4l}^{(m)} R_{1,2l}^{(3)}(-ic,i\xi)\Big]. \quad (56b)$$

The general form of the solution to the linear system of equations obtained by imposing the boundary conditions is:

$$\begin{cases} \widetilde{c}_{rl}^{(m)} = \dfrac{\Delta\widetilde{c}_{rl}^{(m)}}{\Delta^{(m)}}, & r = 1,3,4; \\ \widetilde{d}_{sl}^{(m)} = \dfrac{\Delta\widetilde{d}_{sl}^{(m)}}{\Delta^{(m)}}, & s = 2,\ldots,4; \end{cases} \quad (57)$$

where $\widetilde{c}_{2l}^{(m)} = -G_{2l}(\xi_1)$ and the determinant of the coefficients $\Delta^{(m)}$ is still given by (63a). The other determinants are reported in Table 8.

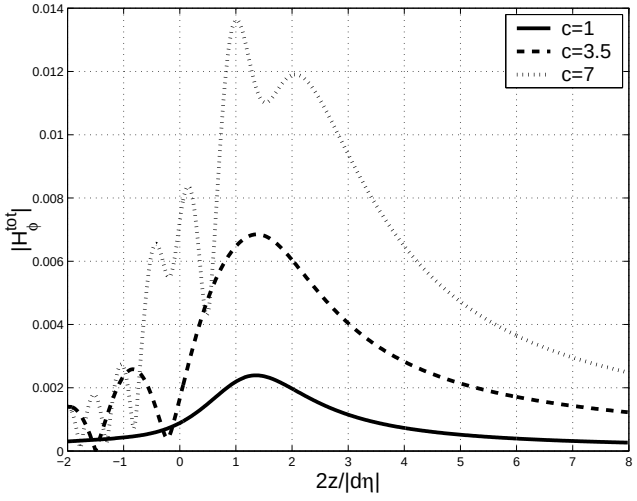

Figure 3. Electric dipole in medium 1, located at $(\eta_0 = 1, \xi_0 = 1.5)$. Total magnetic field $|H_\varphi|$ evaluated along the surface $|\eta| = 0.7$ using equations (10), (14a) and (14b) for three different values of c, when $Z_1 = Z_2 = Z_3 = Z_4 = 120\pi$.

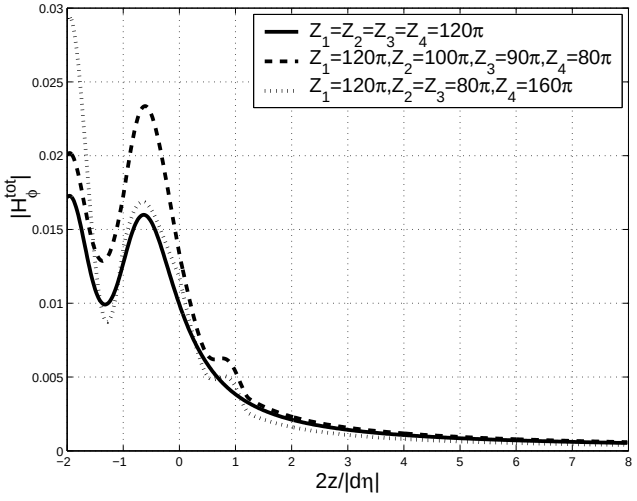

Figure 4. Electric dipole in medium 2, located at $(\eta_0 = -1, \xi_0 = 1.5)$. Total magnetic field $|H_\varphi|$ evaluated along the surface $|\eta| = 0.01$ taking equations (22), (23) and (13) with $c_{1l}^{(e)}$ replacing $a_{1l}^{(e)}$, when $c = 6$. Three different sets of intrinsic impedances for the media have been considered.

5. Numerical Results

The numerical evaluation of the fields was performed using some of the Fortran routines that implement oblate spheroidal radial and angular functions published in *Zhang and Jin* [1996], and, in order to achieve convergence, the acceleration technique reported in *Erricolo* [2003].

The quantities of interest that need to be computed are E_φ or H_φ, when either a magnetic or electric source is considered, respectively. The fields are evaluated along the coordinate lines $|\eta| =$ constant as shown in Fig. 2. Several values of the parameter $c = kd/2$ are considered because c has the physical meaning of the ratio of the aperture size to the wavelength. In all the numerical results, the curved metallic cavity corresponds to the semi-spheroidal coordinate surface $\xi_1 = 2$, whereas the lower and the upper faces of the diaphragm are given by $\xi_2 = 1$ and $\xi_3 = 1.25$ respectively. Also, the dipole sources in medium 1 and 2 are located along the z axis at $(\eta_0 = \pm 1, \xi_0 = 1.5)$, thus preventing the numerical computation of the field at the location of the source. All the diagrams show the field quantities as a function of the dimensionless variable $2z/(d|\eta|)$ since this quantity corresponds to ξ when $z \geq 0$, and to $-\xi$ when $z < 0$. In fact, by looking at (1), it is apparent that η changes sign across the plane $z = 0$, so that $2z/(d|\eta|)$ is positive outside the cavity and negative inside the cavity. Furthermore, the field radiated by the dipoles has been computed directly using the exact expression in spherical coordinates.

In Fig. 3 it is shown the total magnetic field $|H_\varphi|$ given by (10), (14a) and (14b) due to an electric dipole located in the unbounded medium. The magnitude of the total magnetic field $|H_\varphi|$ when the source is an electric dipole located in medium 2 is presented in Fig.4; in particular the behavior of the field in the media 2, 3 and 4 is computed with equations (22), and (23) for $h = 3, 4$, and, in the unbounded medium, equation (13) with the modal coefficient $a_{1l}^{(e)}$ replaced by $c_{1l}^{(e)}$. The plots of Figs. 3 and 4 show that $|H_\varphi|$ has a zero derivative in the neighborhood of the conducting wall at the bottom of the cavity. This behavior suggests that the normal derivative of $|H_\varphi|$ is zero at the wall, thus satisfying the boundary condition at the conducting interface. In Fig.5, it is plotted the total electric field $|E_\varphi|$ when the source is a magnetic dipole in medium 2. In this case, the total electric field is evaluated along three different surfaces $|\eta| =$ constant using equations (47) through (49). The contour plot of the magnitude of the electric field due to a magnetic dipole located in medium 1 is shown in Fig. 6. The equations used to evaluate the magnitude of the total electric field in

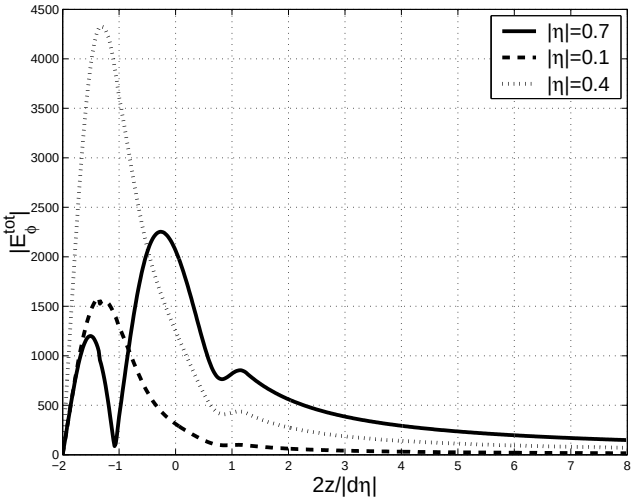

Figure 5. Magnetic dipole in medium 2, located at $(\eta_0 = -1, \xi_0 = 1.5)$. Total electric field $|E_\varphi|$ evaluated along three different surfaces $|\eta| =$ constant using equations (47) through (49) , when $Z_1 = 120\pi$, $Z_2 = 100\pi$, $Z_3 = Z_4 = 80\pi$, and $c = 4$.

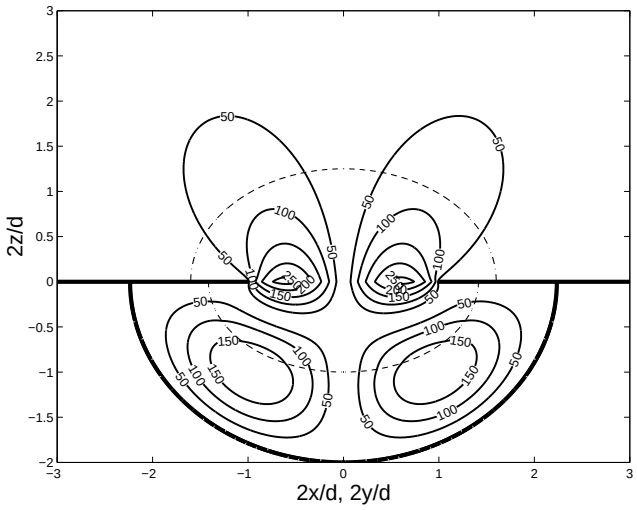

Figure 6. Magnetic dipole in medium 1, located at $(\eta_0 = 1, \xi_0 = 1.5)$. Contour plot of the electric field $|E_\varphi|$ evaluated using equations (41b) and (41a) with $h = 4$ for $z < 0$, while using (40) and (58) for $z > 0$. Also $c = 3$, $Z_1 = Z_3 = 120\pi$, $Z_2 = 100\pi$, and $Z_4 = 80\pi$.

medium 2 and 4 are (41b) and (41a) with $h = 4$, respectively. Since the magnitude of the scattered field in media 1 and 3 is smaller than the geometrical optics field, only equation (40) for the diffracted field was computed in the unbounded medium, while, for medium 3, the following expression was evaluated, with $Z_1 = Z_3$:

$$E^s_{3\varphi} = -\frac{4k^2 Z_3}{\sqrt{\xi_0^2+1}} \sum_{l=1}^{\infty} \frac{(-1)^l S_{1,2l}(-ic,\eta)}{\widetilde{\rho}_{1,2l}\widetilde{N}_{1,2l}} \times \left[\left(b^{(m)}_{3l} - R^{(3)}_{1,2l}(-ic, i\xi_0) \right) R^{(1)}_{1,2l}(-ic, i\xi) + a^{(m)}_{3l} R^{(3)}_{1,2l}(-ic, i\xi) \right]. \quad (58)$$

All the computations regarding the series expansions for the fields were carried out by applying Shanks transform (see *Singh et al.* [1990]) to both the real and imaginary part. Convergence was achieved within the first 40 terms. Each curve representing an electric or magnetic field was evaluated in 150 points along the coordinate lines $|\eta| =$ constant; in particular, the variable $2z/|\eta d|$ takes the values from $-\xi_0$ to $3\xi_0$. The computation time for each of the following figure, except for the contour plot, has been less than 1min. All simulations were run on a personal computer at 3.06 GHz.

6. Conclusion

Exact analytical and numerical results for an electromagnetic boundary-value problem involving a cavity, sharp curved edges, a diaphragm and four isorefractive media were presented.

These results represent the solution of a new canonical problem and, therefore, are important because they enrich the list of geometries for which a frequency-domain exact solutions are known.

Additionally, these results are important to validate computational electromagnetic software. For example, one may consider to use these new analytical results to check the behavior of a purely numerical solution in proximity of the metallic sharp edge.

The analysis performed in this paper could be extended to a primary source that is a uniform (electric or magnetic) current loop located on the symmetry axis and axially oriented.

Acknowledgments. This work was supported by the U.S. Department of Defense and the US Air Force Office of Scientific Research under MURI grant F49620-01-1-0436. Additionally, this work was supported in part by a grant of computer time from the DOD High Performance Computing Modernization Program at ASC.

References

Berardi, C., D. Erricolo, and P. Uslenghi (2004), Exact dipole radiation for an oblate spheroidal cavity filled with isorefractive material and aperture-coupled to a half space, *IEEE Trans. Antennas Propagat.*, *52*(9), 2205–2213.

Bowman, J. J., T. B. A. Senior, and P. L. E. Uslenghi (1987), *Electromagnetic and Acoustic Scattering by Simple Shapes*, Hemisphere Publishing Corporation, New York.

Daniele, V., and P. Uslenghi (1999), Closed-form solution for a line source at the edge of an isorefractive wedge, *IEEE Trans. Antennas Propagat.*, *47*(4), 764–765.

Erricolo, D. (2003), Acceleration of the convergence of series containing Mathieu functions using Shanks transformation, *IEEE Antennas Wireless Propagat. Lett.*, *2*, 58–61.

Erricolo, D., and P. Uslenghi (2005a), Exact Radiation for Dipoles on Metallic Spheroids at the Interface Between Isorefractive Half-Spaces, *IEEE Trans. Antennas Propagat.*, *53*(12), 3974–3981.

Erricolo, D., and P. L. E. Uslenghi (2004), Exact radiation and scattering for an elliptic metal cylinder at the interface between isorefractive half-spaces, *IEEE Trans. Antennas Propagat.*, *52*(9), 2214–2225.

Erricolo, D., and P. L. E. Uslenghi (2005b), Penetration, radiation, and scattering for a cavity-backed gap in a corner, *IEEE Trans. Antennas Propagat.*, *53*(8), 2738–2748.

Erricolo, D., M. Lockard, C. Butler, and P. Uslenghi (2005a), Currents on conducting surfaces of a semielliptical-channel-backed slotted screen in an isorefractive environment, *IEEE Trans. Antennas Propagat.*, *53*(7), 2350–2356.

Erricolo, D., M. D. Lockard, C. M. Butler, and P. L. E. Uslenghi (2005b), Numerical analysis of penetration, radiation, and scattering for a 2D slotted semielliptical channel filled with isorefractive material, *PIER*, *53*, 69–89.

Erricolo, D., P. Uslenghi, B. Elnour, and F. Mioc (2005c), Scattering by a blade on a metallic plane, *Electromagnetics*, *26*(1), 57–71.

Erricolo, D., P. Uslenghi, and M. Valentino (2005d), Exact Analysis of a Spheroidal Cavity with a Circular Aperture in a Ground Plane Covered by an Isorefractive Lens, in *Proc. Intl. Conf. on Electromagnetics in Advanced Applications (ICEAA'05)*, pp. 903–906, Turin, Italy.

Flammer, C. (1957), *Spheroidal wave functions*, Stanford University Press.

Jones, D. S. (1986), *Acoustic and electromagnetic waves*, Oxford.

Knockaert, L., F. Olyslager, and D. DeZutter (1997), The diaphanous wedge, *IEEE Trans. Antennas Propagat.*, *45*(9), 1374–1381.

Roy, S., and P. Uslenghi (1997), Exact scattering for axial incidence on an isorefractive paraboloid, *IEEE Trans. Antennas Propagat.*, *45*(10), 1563.

Table 1. Electric dipole in the unbounded medium: determinants.

$$\Delta^{(e)} = [N(0)(1+\zeta_{34})(N_{2l+1}(\xi_3)M_{2l+1}(\xi_3) - \zeta_{13}) - N_{2l+1}(\xi_3)(1-\zeta_{13})][M_{2l+1}(\xi_2) - M_{2l+1}(\xi_1) - \zeta_{42}M_{2l+1}(\xi_2)\times (1-M_{2l+1}(\xi_1)N_{2l+1}(\xi_2))] + \zeta_{34}[N_{2l+1}(\xi_3)M_{2l+1}(\xi_3) - \zeta_{13}][N_{2l+1}(\xi_2)(M_{2l+1}(\xi_1) - M_{2l+1}(\xi_2)) + \zeta_{42}(1 - M_{2l+1}(\xi_1)N_{2l+1}(\xi_2)$$ (59a)

$$\Delta a_{1l}^{(e)} = [M_{2l+1}(\xi_3)N(0)(1+\zeta_{34})(1-\zeta_{13}) + \zeta_{13}M_{2l+1}(\xi_3)N_{2l+1}(\xi_3) - 1]\,[M_{2l+1}(\xi_2) - M_{2l+1}(\xi_1) - \zeta_{42}M_{2l+1}(\xi_2)\times (1 - M_{2l+1}(\xi_1)N_{2l+1}(\xi_2))] + M_{2l+1}(\xi_3)\zeta_{34}(1-\zeta_{13})\,[N_{2l+1}(\xi_2)(M_{2l+1}(\xi_1) - M_{2l+1}(\xi_2)) + \zeta_{42}(1 - M_{2l+1}(\xi_1)N_{2l+1}(\xi_2))]\,;$$ (59b)

$$\Delta a_{2l}^{(e)} = \frac{M_{2l+1}(\xi_1)\Delta^{(e)}}{R^{(3)}_{1,2l+1}(-ic, i\xi_0)};$$ (59c)

$$\Delta a_{3l}^{(e)} = -\Delta a_{4l}^{(e)} = [M_{2l+1}(\xi_2) - M_{2l+1}(\xi_1) - \zeta_{42}M_{2l+1}(\xi_2)(1 - N_{2l+1}(\xi_2)M_{2l+1}(\xi_1))][N_{2l+1}(\xi_3)M_{2l+1}(\xi_3) - 1];$$ (59d)

$$\Delta b_{2l}^{(e)} = [1 - N_{2l+1}(\xi_2)M_{2l+1}(\xi_2)][1 - M_{2l+1}(\xi_3)N_{2l+1}(\xi_3)];$$ (59e)

$$\Delta b_{3l}^{(e)} = (1 - M_{2l+1}(\xi_3)N_{2l+1}(\xi_3))\{[N(0)(1+\zeta_{34})(M_{2l+1}(\xi_2) - M_{2l+1}(\xi_1) - \zeta_{42}M_{2l+1}(\xi_2)\times (1 - M_{2l+1}(\xi_1)N_{2l+1}(\xi_2))] - \zeta_{34}[N_{2l+1}(\xi_2)(M(\xi_2) - M_{2l+1}(\xi_1)) - \zeta_{42}(1 - N_{2l+1}(\xi_2)M_{2l+1}(\xi_1))]\};$$ (59f)

$$\Delta b_{4l}^{(e)} = [1 - M_{2l+1}(\xi_3)N_{2l+1}(\xi_3)][\zeta_{42}(1 - N_{2l+1}(\xi_2)M_{2l+1}(\xi_1)) + N_{2l+1}(\xi_2)(M_{2l+1}(\xi_1) - M_{2l+1}(\xi_2))];$$ (59g)

(59h)

Singh, S., W. F. Richards, J. R. Zinecker, and D. R. Wilton (1990), Accelerating the convergence of series representing the free space periodic green's function, *IEEE Trans. Antennas Propagat.*, *38*(12), 1958–1962.

Uslenghi, P. (1997a), Exact solution for a penetrable wedge structure, *IEEE Trans. Antennas Propagat.*, *45*(1), 179.

Uslenghi, P. (1997b), Exact scattering by isorefractive bodies, *IEEE Trans. Antennas Propagat.*, *45*(9), 1382–1385.

Uslenghi, P. (2000), Exact geometrical optics solution for an isorefractive wedge structure, *IEEE Trans. Antennas Propagat.*, *48*(2), 335–336.

Uslenghi, P. (2004a), Exact penetration, radiation and scattering for a slotted semielliptical channel filled with isorefractive material, *IEEE Trans. Antennas Propagat.*, *52*(6), 1473–1480.

Uslenghi, P. (2004b), Exact geometrical optics scattering from a tri-sector isorefractive wedge structure, *IEEE Antennas Wireless Propagat. Lett.*, *3*, 94–95.

Uslenghi, P., and R. Zich (1998), Radiation and scattering from isorefractive bodies of revolution, *IEEE Trans. Antennas Propagat.*, *46*(11), 1606–1611.

Valentino, M. (2005), Elliptic and spheroidal shapes with a cavity, a lens and isorefractive media: EM analysis and evaluation, Master's thesis, University of Illinois at Chicago, USA.

Valentino, M., and D. Erricolo (2006), Exact 2D scattering from a slot in a ground plane backed by a semielliptical cavity and covered with an isorefractive diaphragm, *Radio Sci.*, this issue.

Zhang, S., and J.-M. Jin (1996), *Computation of Special Functions*, Wiley, New York.

M. Valentino, Department of Electrical and Computer Engineering, University of Illinois at Chicago, 851 S. Morgan Street, Chicago, IL, USA. (marval83@libero.it)

(Received _____.)

Table 2. Electric dipole in the material filling the cavity.

$$\Delta c_{1l}^{(e)} = \zeta_{13}\zeta_{34}\zeta_{42}\left[1 - M_{2l+1}(\xi_3)N_{2l+1}(\xi_3)\right]\Big[(M_{2l+1}(\xi_2) - M_{2l+1}(\xi_1))\Big(N_{2l+1}(\xi_2)R_{1,2l+1}^{(1)}(-ic, i\xi_0) - R_{1,2l+1}^{(3)}(-ic, i\xi_0)\Big) + (1 - M_{2l+1}(\xi_1)N_{2l+1}(\xi_2))\Big(M_{2l+1}(\xi_2)R_{1,2l+1}^{(3)}(-ic, i\xi_0) - R_{1,2l+1}^{(1)}(-ic, i\xi_0)\Big)\Big]; \tag{60a}$$

$$\Delta c_{2l}^{(e)} = -\frac{\Big[\Delta d_{2l}^{(e)} + R_{1,2l+1}^{(1)}(-ic, i\xi_0)\Big]}{M_{2l+1}(\xi_1)}; \tag{60b}$$

$$\Delta c_{3l}^{(e)} = -\Delta c_{4l}^{(e)} = \zeta_{34}\zeta_{42}\left[\zeta_{13} - M_{2l+1}(\xi_3)N_{2l+1}(\xi_3)\right]\Big[(M_{2l+1}(\xi_2) - M_{2l+1}(\xi_1))\Big(N_{2l+1}(\xi_2)R_{1,2l+1}^{(1)}(-ic, i\xi_0) - R_{1,2l+1}^{(3)}(-ic, i\xi_0)\Big) + (1 - M_{2l+1}(\xi_1)N_{2l+1}(\xi_2))\Big(M_{2l+1}(\xi_2)R_{1,2l+1}^{(3)}(-ic, i\xi_0) - R_{1,2l+1}^{(1)}(-ic, i\xi_0)\Big)\Big]; \tag{60c}$$

$$\Delta d_{2l}^{(e)} = [N_{2l+1}(\xi_3)(\zeta_{13} - 1) + N(0)(1 + \zeta_{34})\left(M_{2l+1}(\xi_3)N_{2l+1}(\xi_3) - \zeta_{13}\right)]\Big[R_{1,2l+1}^{(1)}(-ic, i\xi_0) - M_{2l+1}(\xi_2)R_{1,2l+1}^{(3)}(-ic, i\xi_0) + \zeta_{42}M_{2l+1}(\xi_2)\Big(R_{1,2l+1}^{(3)}(-ic, i\xi_0) - N_{2l+1}(\xi_2)\times R_{1,2l+1}^{(1)}(-ic, i\xi_0)\Big)\Big] + \zeta_{34}\left[\zeta_{13} - M_{2l+1}(\xi_3)N_{2l+1}(\xi_3)\right]\Big[N_{2l+1}(\xi_2)\Big(R_{1,2l+1}^{(1)}(-ic, i\xi_0) - M_{2l+1}(\xi_2)\times R_{1,2l+1}^{(3)}(-ic, i\xi_0)\Big) + \zeta_{42}(R_{1,2l+1}^{(3)}(-ic, i\xi_0) - N_{2l+1}(\xi_2)R_{1,2l+1}^{(1)}(-ic, i\xi_0))\Big]; \tag{60d}$$

$$\Delta d_{3l}^{(e)} = \zeta_{34}\zeta_{42}N_{2l+1}(\xi_3)\left[\zeta_{13} - 1\right]\Big[(M_{2l+1}(\xi_2) - M_{2l+1}(\xi_1))\Big(N_{2l+1}(\xi_2)R_{1,2l+1}^{(1)}(-ic, i\xi_0) - R_{1,2l+1}^{(3)}(-ic, i\xi_0)\Big) + (1 - M_{2l+1}(\xi_1)N_{2l+1}(\xi_2))\Big(M_{2l+1}(\xi_2)R_{1,2l+1}^{(3)}(-ic, i\xi_0) - R_{1,2l+1}^{(1)}(-ic, i\xi_0)\Big)\Big]; \tag{60e}$$

$$\Delta d_{4l}^{(e)} = \zeta_{42}\left[N_{2l+1}(\xi_3)(\zeta_{13} - 1) + N(0)(1 + \zeta_{34})(M_{2l+1}(\xi_3)N_{2l+1}(\xi_3) - \zeta_{13})\right]\left[(M_{2l+1}(\xi_2) - M_{2l+1}(\xi_1))\left(N_{2l+1}(\xi_2)\times R_{1,2l+1}^{(1)}(-ic, i\xi_0) - R_{1,2l+1}^{(3)}(-ic, i\xi_0)\Big) + (1 - M_{2l+1}(\xi_1)N_{2l+1}(\xi_2))\Big(M_{2l+1}(\xi_2)R_{1,2l+1}^{(3)}(-ic, i\xi_0) - R_{1,2l+1}^{(1)}(-ic, i\xi_0)\Big)\right]. \tag{60f}$$

Table 3. Electric dipole in medium 3.

$$\Delta\widetilde{a}^{(e)}_{1l} = \zeta_{13}\left[M_{2l+1}(\xi_3)N_{2l+1}(\xi_3)-1\right]\Big\{\Big[(1+\zeta_{34})N(0)R^{(1)}_{1,2l+1}(-ic,i\xi_0)-R^{(3)}_{1,2l+1}(-ic,i\xi_0)\Big]\times$$
$$\left[M_{2l+1}(\xi_2)-M_{2l+1}(\xi_1)-\zeta_{42}M_{2l+1}(\xi_2)\left(1-M_{2l+1}(\xi_1)N_{2l+1}(\xi_2)\right)\right]-\zeta_{34}R^{(1)}_{1,2l+1}(-ic,i\xi_0)$$
$$\left[(M_{2l+1}(\xi_2)-M_{2l+1}(\xi_1))N_{2l+1}(\xi_2)-\zeta_{42}(1-M_{2l+1}(\xi_1)N_{2l+1}(\xi_2))\right]\Big\}; \tag{61a}$$

$$\Delta\widetilde{a}^{(e)}_{3l} = -\Delta\widetilde{a}^{(e)}_{4l} = \Big[R^{(1)}_{1,2l+1}(-ic,i\xi_0)N_{2l+1}(\xi_3)(1-\zeta_{13})+R^{(3)}_{1,2l+1}(-ic,i\xi_0)\left(\zeta_{13}-M_{2l+1}(\xi_3)N_{2l+1}(\xi_3)\right)\Big]\times$$
$$\left[M_{2l+1}(\xi_2)-M_{2l+1}(\xi_1)-\zeta_{42}M_{2l+1}(\xi_2)\left(1-M_{2l+1}(\xi_1)N_{2l+1}(\xi_2)\right)\right]; \tag{61b}$$

$$\Delta\widetilde{b}^{(e)}_{2l} = \Big[R^{(1)}_{1,2l+1}(-ic,i\xi_0)N_{2l+1}(\xi_3)(\zeta_{13}-1)+R^{(3)}_{1,2l+1}(-ic,i\xi_0)\left(M_{2l+1}(\xi_3)N_{2l+1}(\xi_3)\right)-\zeta_{13}\Big]\times$$
$$\left[1-M_{2l+1}(\xi_2)N_{2l+1}(\xi_2)\right]; \tag{61c}$$

$$\Delta\widetilde{b}^{(e)}_{3l} = \left[\zeta_{13}-1\right]\Big\{\Big[R^{(1)}_{1,2l+1}(-ic,i\xi_0)N_{2l+1}(\xi_3)N_{2l+1}(\xi_0)(1+\zeta_{34})-R^{(3)}_{1,2l+1}(-ic,i\xi_0)N_{2l+1}(\xi_3)\Big]\times$$
$$\left[M_{2l+1}(\xi_2)-M_{2l+1}(\xi_1)-\zeta_{42}M_{2l+1}(\xi_2)\left(1-M_{2l+1}(\xi_1)N_{2l+1}(\xi_2)\right)\right]-\zeta_{34}N_{2l+1}(\xi_3)R^{(1)}_{1,2l+1}(-ic,i\xi_0)\times$$
$$\left[(M_{2l+1}(\xi_2)-M_{2l+1}(\xi_1))N_{2l+1}(\xi_2)-\zeta_{42}(1-M_{2l+1}(\xi_1)N_{2l+1}(\xi_2))\right]\Big\}; \tag{61d}$$

$$\Delta\widetilde{b}^{(e)}_{4l} = \Big[R^{(1)}_{1,2l+1}(-ic,i\xi_0)N_{2l+1}(\xi_3)(\zeta_{13}-1)+R^{(3)}_{1,2l+1}(-ic,i\xi_0)\left(M_{2l+1}(\xi_3)N_{2l+1}(\xi_3)\right)-\zeta_{13}\Big]\times$$
$$\left[(M_{2l+1}(\xi_2)-M_{2l+1}(\xi_1))N_{2l+1}(\xi_2)-\zeta_{42}(1-M_{2l+1}(\xi_1)N_{2l+1}(\xi_2))\right]. \tag{61e}$$

Table 4. Electric dipole in medium 4.

$$\Delta\widetilde{c}^{(e)}_{1l} = \zeta_{13}\zeta_{34}\left[M_{2l+1}(\xi_3)N_{2l+1}(\xi_3)-1\right]\Big\{R^{(3)}_{1,2l+1}(-ic,i\xi_0)\left[M_{2l+1}(\xi_2)-M_{2l+1}(\xi_1)-\zeta_{42}M_{2l+1}(\xi_2)\left(1-M_{2l+1}(\xi_1)N_{2l+1}(\xi_2)\right)\right]-$$
$$R^{(1)}_{1,2l+1}(-ic,i\xi_0)\left[(M_{2l+1}(\xi_2)-M_{2l+1}(\xi_1))N_{2l+1}(\xi_2)-\zeta_{42}(1-M_{2l+1}(\xi_1)N_{2l+1}(\xi_2))\right]\Big\}; \tag{62a}$$

$$\Delta\widetilde{c}^{(e)}_{2l} = -M_{2l+1}(\xi_1)\Delta^{(e)}; \tag{62b}$$

$$\Delta\widetilde{c}^{(e)}_{3l} = -\Delta\widetilde{c}^{(e)}_{4l} = \zeta_{34}\left[M_{2l+1}(\xi_3)N_{2l+1}(\xi_3)-\zeta_{13}\right]\Big\{R^{(3)}_{1,2l+1}(-ic,i\xi_0)\left[M_{2l+1}(\xi_2)-M_{2l+1}(\xi_1)-\zeta_{42}M_{2l+1}(\xi_2)\times\right.$$
$$\left.(1-M_{2l+1}(\xi_1)N_{2l+1}(\xi_2))\right]-R^{(1)}_{1,2l+1}(-ic,i\xi_0)\left[(M_{2l+1}(\xi_2)-M_{2l+1}(\xi_1))N_{2l+1}(\xi_2)-\zeta_{42}(1-M_{2l+1}(\xi_1)N_{2l+1}(\xi_2))\right]\Big\}; \tag{62c}$$

$$\Delta\widetilde{d}^{(e)}_{2l} = \left[1-M_{2l+1}(\xi_2)N_{2l+1}(\xi_2)\right]\Big\{(\zeta_{13}-1)N_{2l+1}(\xi_3)R^{(1)}_{1,2l+1}(-ic,i\xi_0)+\left[M_{2l+1}(\xi_3)N_{2l+1}(\xi_3)-1\right]\times$$
$$\Big[N(0)(1+\zeta_{34})R^{(1)}_{1,2l+1}(-ic,i\xi_0)-\zeta_{34}R^{(3)}_{1,2l+1}(-ic,i\xi_0)\Big]\Big\}; \tag{62d}$$

$$\Delta\widetilde{d}^{(e)}_{3l} = \zeta_{34}N_{2l+1}(\xi_3)\left[\zeta_{13}-1\right]\Big\{R^{(3)}_{1,2l+1}(-ic,i\xi_0)\left[M_{2l+1}(\xi_2)-M_{2l+1}(\xi_1)-\zeta_{42}M_{2l+1}(\xi_2)\left(1-M_{2l+1}(\xi_1)N_{2l+1}(\xi_2)\right)\right]-$$
$$R^{(1)}_{1,2l+1}(-ic,i\xi_0)\left[(M_{2l+1}(\xi_2)-M_{2l+1}(\xi_1))N_{2l+1}(\xi_2)-\zeta_{42}(1-M_{2l+1}(\xi_1)N_{2l+1}(\xi_2))\right]\Big\}; \tag{62e}$$

$$\Delta\widetilde{d}^{(e)}_{4l} = \left[(M_{2l+1}(\xi_1)-M_{2l+1}(\xi_2))N_{2l+1}(\xi_2)+\zeta_{42}(1-M_{2l+1}(\xi_1)N_{2l+1}(\xi_2))\right]\Big\{R^{(1)}_{1,2l+1}(-ic,i\xi_0)\left[N_{2l+1}(\xi_3)(\zeta_{13}-1)+\right.$$
$$\left.N(0)(1+\zeta_{34})\left(M_{2l+1}(\xi_3)N_{2l+1}(\xi_3)\right)-\zeta_{13}\right]-\zeta_{34}R^{(3)}_{1,2l+1}(-ic,i\xi_0)\left[M_{2l+1}(\xi_3)N_{2l+1}(\xi_3)-\zeta_{13}\right]\Big\}. \tag{62f}$$

Table 5. Magnetic dipole in the unbounded medium: determinants.

$$\Delta^{(m)} = [F(0)(1-\zeta_{13}) + (1+\zeta_{34})(\zeta_{13}F_{2l}(\xi_3) - G_{2l}(\xi_3))]\,[\zeta_{42}F_{2l}(\xi_2)(F_{2l}(\xi_1) - G_{2l}(\xi_2)) + F_{2l}(\xi_2)\times (G_{2l}(\xi_2) - G_{2l}(\xi_1))] + \zeta_{34}F(0)\,[G_{2l}(\xi_3) - \zeta_{13}F_{2l}(\xi_3)]\,[\zeta_{42}(F_{2l}(\xi_1) - G_{2l}(\xi_2)) + G_{2l}(\xi_2) - G_{2l}(\xi_1)]\,; \tag{63a}$$

$$\Delta a_{1l}^{(m)} = [F(0)(F_{2l}(\xi_3) - \zeta_{13}G_{2l}(\xi_3)) + F_{2l}(\xi_3)G_{2l}(\xi_3)(1+\zeta_{34})(\zeta_{13}-1)]\,[\zeta_{42}F_{2l}(\xi_2)(F_{2l}(\xi_1) - G_{2l}(\xi_2)) + F_{2l}(\xi_2)(G_{2l}(\xi_2) - G_{2l}(\xi_1))] + \zeta_{34}F(0)F_{2l}(\xi_3)G_{2l}(\xi_3)(1-\zeta_{13})\,[\zeta_{42}(F_{2l}(\xi_1) - G_{2l}(\xi_2)) + G_{2l}(\xi_2) - G_{2l}(\xi_1)]\,; \tag{63b}$$

$$\Delta a_{2l}^{(m)} = G_{2l}(\xi_1)\Delta^{(m)}/R_{1,2l}^{(3)}(-ic, i\xi_0); \tag{63c}$$

$$\Delta a_{3l}^{(m)} = -\,\zeta_{34}^{-1}\Delta a_{4l}^{(m)} = \zeta_{13}F(0)(F_{2l}(\xi_3) - G_{2l}(\xi_3))\,[\zeta_{42}F_{2l}(\xi_2)(F_{2l}(\xi_1) - G_{2l}(\xi_2)) + F_{2l}(\xi_2)(G_{2l}(\xi_2) - G_{2l}(\xi_1))]\,; \tag{63d}$$

$$\Delta b_{2l}^{(m)} = \zeta_{13}\zeta_{34}\zeta_{42}F(0)\,[G_{2l}(\xi_3) - F_{2l}(\xi_3)]\,[F_{2l}(\xi_2) - G_{2l}(\xi_2)]\,; \tag{63e}$$

$$\Delta b_{3l}^{(m)} = \zeta_{13}(1+\zeta_{34})(G_{2l}(\xi_3) - F_{2l}(\xi_3))\,[\zeta_{42}F_{2l}(\xi_2)(F_{2l}(\xi_1) - G_{2l}(\xi_2)) + F_{2l}(\xi_2)(G_{2l}(\xi_2) - G_{2l}(\xi_1))] + \zeta_{34}\zeta_{13}F(0)(F_{2l}(\xi_3) - G_{2l}(\xi_3))\,[\zeta_{42}(F_{2l}(\xi_1) - G_{2l}(\xi_2)) + G_{2l}(\xi_2) - G_{2l}(\xi_1)]\,; \tag{63f}$$

$$\Delta b_{4l}^{(m)} = \zeta_{13}\zeta_{34}F(0)\,[G_{2l}(\xi_3) - F_{2l}(\xi_3)]\,[G_{2l}(\xi_1) - G_{2l}(\xi_2) - \zeta_{42}(G_{2l}(\xi_1) - F_{2l}(\xi_2))]\,. \tag{63g}$$

Table 6. Magnetic dipole in the material filling the cavity: determinants.

$$\Delta c_{1l}^{(m)} = F(0)\,[F_{2l}(\xi_3) - G_{2l}(\xi_3)]\left[(G_{2l}(\xi_1) - F_{2l}(\xi_2))\left(R_{1,2l}^{(3)}(-ic, i\xi_0)G_{2l}(\xi_2) - R_{1,2l}^{(1)}(-ic, i\xi_0)\right) + (G_{2l}(\xi_2) - G_{2l}(\xi_1))\left(R_{1,2l}^{(3)}(-ic, i\xi_0)F_{2l}(\xi_2) - R_{1,2l}^{(1)}(-ic, i\xi_0)\right)\right]; \tag{64a}$$

$$\Delta c_{2l}^{(m)} = -\left[G_{2l}(\xi_1)\Delta d_{2l}^{(m)} + R_{1,2l}^{(1)}(-ic, i\xi_0)\right]; \tag{64b}$$

$$\Delta c_{3l}^{(m)} = -\,\zeta_{34}^{-1}\Delta c_{4l}^{(m)} = F(0)\,[\zeta_{13}F_{2l}(\xi_3) - G_{2l}(\xi_3)]\left[(G_{2l}(\xi_1) - F_{2l}(\xi_2))\left(R_{1,2l}^{(3)}(-ic, i\xi_0)G_{2l}(\xi_2) - R_{1,2l}^{(1)}(-ic, i\xi_0)\right) + (G_{2l}(\xi_2) - G(\xi_1))\left(R_{1,2l}^{(3)}(-ic, i\xi_0)F_{2l}(\xi_2) - R_{1,2l}^{(1)}(-ic, i\xi_0)\right)\right]; \tag{64c}$$

$$\Delta d_{2l}^{(m)} = [F(0)(1-\zeta_{13}) + (1+\zeta_{34})\,(\zeta_{13}F_{2l}(\xi_3) - G_{2l}(\xi_3))]\times \left[\zeta_{42}G_{2l}(\xi_2)\left(F_{2l}(\xi_2)R_{1,2l}^{(3)}(-ic, i\xi_0) - R_{1,2l}^{(1)}(-ic, i\xi_0)\right) + F_{2l}(\xi_2)\left(R_{1,2l}^{(1)}(-ic, i\xi_0) - G_{2l}(\xi_2)\times R_{1,2l}^{(3)}(-ic, i\xi_0)\right)\right] + \zeta_{34}F(0)\,[G_{2l}(\xi_3) - \zeta_{13}F_{2l}(\xi_3)]\left[\zeta_{42}\left(F_{2l}(\xi_2)R_{1,2l}^{(3)}(-ic, i\xi_0) - R_{1,2l}^{(1)}(-ic, i\xi_0)\right) + \left(R_{1,2l}^{(1)}(-ic, i\xi_0) - G_{2l}(\xi_2)R_{1,2l}^{(3)}(-ic, i\xi_0)\right)\right]; \tag{64d}$$

$$\Delta d_{3l}^{(m)} = F(0)\,[1-\zeta_{13}]\left[(G_{2l}(\xi_1) - F_{2l}(\xi_2))\left(R_{1,2l}^{(3)}(-ic, i\xi_0)G_{2l}(\xi_2) - R_{1,2l}^{(1)}(-ic, i\xi_0)\right) + (G_{2l}(\xi_2) - G_{2l}(\xi_1))\left(R_{1,2l}^{(3)}(-ic, i\xi_0)F_{2l}(\xi_2) - R_{1,2l}^{(1)}(-ic, i\xi_0)\right)\right]; \tag{64e}$$

$$\Delta d_{4l}^{(m)} = [F(0)(1-\zeta_{13}) + (1+\zeta_{34})\,(\zeta_{13}F_{2l}(\xi_3) - G_{2l}(\xi_3))]\left[(G_{2l}(\xi_1) - F_{2l}(\xi_2))\left(R_{1,2l}^{(3)}(-ic, i\xi_0)G_{2l}(\xi_2) - R_{1,2l}^{(1)}(-ic, i\xi_0)\right) + (G_{2l}(\xi_2) - G(\xi_1))\left(R_{1,2l}^{(3)}(-ic, i\xi_0)F_{2l}(\xi_2) - R_{1,2l}^{(1)}(-ic, i\xi_0)\right)\right]. \tag{64f}$$

Table 7. Magnetic dipole in medium 3: determinants.

$$\Delta\widetilde{a}^{(m)}_{1l} = [G_{2l}(\xi_3) - F_{2l}(\xi_3)] \Big\{ \Big[R^{(3)}_{1,2l}(-ic, i\xi_0)F(0) - (1+\zeta_{34})R^{(1)}_{1,2l}(-ic, i\xi_0) \Big] \times [\zeta_{42}G_{2l}(\xi_2)(G_{2l}(\xi_1) - F_{2l}(\xi_2)) + F_{2l}(\xi_2)(G_{2l}(\xi_2) - G_{2l}(\xi_1))] + \zeta_{34}R^{(1)}_{1,2l}(-ic, i\xi_0)F(0)\times [\zeta_{42}(G_{2l}(\xi_1) - F_{2l}(\xi_2) + G_{2l}(\xi_2) - G_{2l}(\xi_1))] \Big\}; \tag{65a}$$

$$\Delta\widetilde{a}^{(m)}_{3l} = -\zeta^{-1}_{34}\Delta\widetilde{a}^{(m)}_{4l} = F(0)\left[\zeta_{42}G_{2l}(\xi_2)(G_{2l}(\xi_1) - F_{2l}(\xi_2)) + F_{2l}(\xi_2)(G_{2l}(\xi_2) - G_{2l}(\xi_1))\right] \times \Big[R^{(1)}_{1,2l}(-ic, i\xi_0)(\zeta_{13} - 1) + R^{(3)}_{1,2l}(-ic, i\xi_0)\left(G_{2l}(\xi_3) - \zeta_{13}F_{2l}(\xi_3)\right) \Big]; \tag{65b}$$

$$\Delta\widetilde{b}^{(m)}_{2l} = \zeta_{34}\zeta_{42}F(0)\Big[R^{(1)}_{1,2l}(-ic, i\xi_0)(1-\zeta_{13}) + R^{(3)}_{1,2l}(-ic, i\xi_0)(\zeta_{13}P(\xi_3) - Q(\xi_3)) \Big] \times [F_{2l}(\xi_2) - G_{2l}(\xi_2)]; \tag{65c}$$

$$\Delta\widetilde{b}^{(m)}_{3l} = (\zeta_{13}-1)\Big\{ \Big[F(0)R^{(3)}_{1,2l}(-ic, i\xi_0) - (1+\zeta_{34}) \Big] [\zeta_{42}G_{2l}(\xi_2)(G_{2l}(\xi_1) - F_{2l}(\xi_2)) + F_{2l}(\xi_2)\times (G_{2l}(\xi_2) - G_{2l}(\xi_1))] + \zeta_{34}F(0)R^{(1)}_{1,2l}(-ic, i\xi_0)\left[\zeta_{42}(G_{2l}(\xi_1) - F_{2l}(\xi_2) + G_{2l}(\xi_2) - G_{2l}(\xi_1))\right] \Big\}; \tag{65d}$$

$$\Delta\widetilde{b}^{(m)}_{4l} = P(0)\zeta_{34}\left[\zeta_{42}(G_{2l}(\xi_1) - F_{2l}(\xi_2) + G_{2l}(\xi_2) - G_{2l}(\xi_1))\right] \times \Big[R^{(3)}_{1,2l}(-ic, i\xi_0)(Q(\xi_3) - \zeta_{13}P(\xi_3)) + R^{(1)}_{1,2l}(-ic, i\xi_0)(1-\zeta_{13}) \Big]. \tag{65e}$$

Table 8. Magnetic dipole in medium 4: determinants.

$$\Delta\widetilde{c}^{(m)}_{1l} = F(0)\left[F_{2l}(\xi_3) - G_{2l}(\xi_3)\right] \Big\{ R^{(3)}_{1,2l}(-ic, i\xi_0)\left[\zeta_{42}G_{2l}(\xi_2)(G_{2l}(\xi_1) - F_{2l}(\xi_2)) + F_{2l}(\xi_2)(G_{2l}(\xi_2) - G_{2l}(\xi_1))\right] \times R^{(3)}_{1,2l}(-ic, i\xi_0)\left[\zeta_{42}(F_{2l}(\xi_2) - G_{2l}(\xi_1)) + G_{2l}(\xi_1) - G_{2l}(\xi_2)\right] \Big\}; \tag{66a}$$

$$\Delta\widetilde{c}^{(m)}_{3l} = -\zeta^{-1}_{34}\Delta\widetilde{c}^{(m)}_{4l} = F(0)\left[\zeta_{13}F_{2l}(\xi_3) - G_{2l}(\xi_3)\right] \Big\{ R^{(3)}_{1,2l}(-ic, i\xi_0)\left[\zeta_{42}G_{2l}(\xi_2)(G_{2l}(\xi_1) - F_{2l}(\xi_2)) + F_{2l}(\xi_2)(G_{2l}(\xi_2) - G_{2l}(\xi_1))\right] + R^{(3)}_{1,2l}(-ic, i\xi_0)\left[\zeta_{42}(F_{2l}(\xi_2) - G_{2l}(\xi_1)) + G_{2l}(\xi_1) - G_{2l}(\xi_2)\right] \Big\}; \tag{66b}$$

$$\Delta\widetilde{d}^{(m)}_{2l} = F(0)\zeta_{42}R^{(1)}_{1,2l}(-ic, i\xi_0)(F_{2l}(\xi_2) - G_{2l}(\xi_2)) + \zeta_{42}\left[\zeta_{13}F_{2l}(\xi_3) - G_{2l}(\xi_3)\right]\left[F_{2l}(\xi_2) - G_{2l}(\xi_2)\right] \times \Big[(1+\zeta_{34})R^{(1)}_{1,2l}(-ic, i\xi_0) - \zeta_{34}F(0)R^{(3)}_{1,2l}(-ic, i\xi_0) \Big]; \tag{66c}$$

$$\Delta\widetilde{d}^{(m)}_{3l} = F(0)(1-\zeta_{13}) \Big\{ R^{(3)}_{1,2l}(-ic, i\xi_0)\left[\zeta_{42}G_{2l}(\xi_2)(G_{2l}(\xi_1) - F_{2l}(\xi_2)) + F_{2l}(\xi_2)(G_{2l}(\xi_2) - G_{2l}(\xi_1))\right] + R^{(3)}_{1,2l}(-ic, i\xi_0)\left[\zeta_{42}(F_{2l}(\xi_2) - G_{2l}(\xi_1)) + G_{2l}(\xi_1) - G_{2l}(\xi_2)\right] \Big\}; \tag{66d}$$

$$\Delta\widetilde{d}^{(m)}_{4l} = \left[\zeta_{42}(F_{2l}(\xi_2) - G_{2l}(\xi_1)) + G_{2l}(\xi_1) - G_{2l}(\xi_2)\right] \Big\{ R^{(1)}_{1,2l}(-ic, i\xi_0)\left[F(0)(1-\zeta_{13}) + (1+\zeta_{34})(\zeta_{13}F_{2l}(\xi_3) - G_{2l}(\xi_3))\right] - \zeta_{34}F(0)R^{(3)}_{1,2l}(-ic, i\xi_0)(\zeta_{13}F_{2l}(\xi_3) - G_{2l}(\xi_3)) \Big\}. \tag{66e}$$